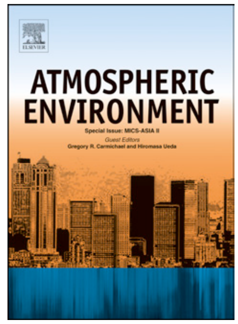

Intercomparision of the capabilities of simplified climate models to project the effects of aviation CO_2 on climate

Arezoo Khodayari, Donald J. Wuebbles, Seth C. Olsen, Jan S. Fuglestvedt, Terje Berntsen, Marianne T. Lund, Ian Waitz, Philip Wolfe, Piers M. Forster, Malte Meinshausen, David S. Lee, Ling L. Lim

PII: S1352-2310(13)00239-2

DOI: 10.1016/j.atmosenv.2013.03.055

Reference: AEA 12067

To appear in: *Atmospheric Environment*

Received Date: 8 October 2012

Revised Date: 23 March 2013

Accepted Date: 27 March 2013

We evaluated carbon cycle in six simple climate models.

We evaluated energy balance model in six simple climate models.

The appropriate carbon cycle for the use in simple climate models (SCMs) was suggested.

The appropriate energy balance model for the use in SCMs was suggested.

Intercomparision of the capabilities of simplified climate models to project the effects of aviation CO_2 on climate

Arezoo Khodayari[a,*], Donald J. Wuebbles[b], Seth C. Olsen[b], Jan S. Fuglestvedt[c], Terje Berntsen[c], Marianne T. Lund[c], Ian Waitz[d], Philip Wolfe[d], Piers M. Forster[e], Malte Meinshausen[f,g], David S. Lee[h] and Ling L. Lim[h]

[a]Department of Civil and Environmental Engineering, University of Illinois at Urbana-Champaign, Urbana, IL 61801
[b]Department of Atmospheric Sciences, University of Illinois at Urbana-Champaign, Urbana, IL 61801,USA
[c]CICERO, Center for International Climate and Environmental Research, Oslo, P.O. Box 1129, Blindern, 0318 Oslo, Norway
[d]Department of Aeronautics and Astronautics, Massachusetts Institute of Technology, Cambridge, MA 02139, USA
[e]School of Earth and Environment, University of Leeds, LS2 9JT, UK
[f]Earth System Analysis, Potsdam Institute for Climate Impact Research (PIK), Potsdam, Germany
[g] School of Earth Sciences, The University of Melbourne, Victoria 3010, Australia
[h]Dalton Research Institute, Manchester Metropolitan University, UK

* Corresponding author. Tel.: 217-979-3837, E-mail address: akhoday2@illinois.edu

Keywords: climate change, simple climate models, carbon cycle, energy balance model

ABSTRACT

This study evaluates the capabilities of the carbon cycle and energy balance treatments relative to the effect of aviation CO_2 emissions on climate in several existing simplified climate models (SCMs) that are either being used or could be used for evaluating the effects of aviation on climate. Since these models are used in policy-related analyses, it is important that the capabilities of such models represent the state of understanding of the science. We compare the Aviation Environmental Portfolio Management Tool (APMT) Impacts climate model, two models used at the Center for International Climate and Environmental Research-Oslo (CICERO-1 and CICERO-2), the Integrated Science Assessment Model (ISAM) model as described in Jain et al. (1994), the simple Linear Climate response model (LinClim) and the Model for the Assessment of Greenhouse-gas Induced Climate Change version 6 (MAGICC6). In this paper we select scenarios to illustrate the behavior of the carbon cycle and energy balance models in these SCMs. This study is not intended to determine the absolute and likely range of the expected climate response in these models but to highlight specific features in model

representations of the carbon cycle and energy balance models that need to be carefully considered in studies of aviation effects on climate. These results suggest that carbon cycle models that use linear impulse-response-functions (IRF) in combination with separate equations describing air-sea and air-biosphere exchange of CO_2 can account for the dominant nonlinearities in the climate system that would otherwise not have been captured with an IRF alone, and hence, produce a close representation of more complex carbon cycle models. Moreover, results suggest that an energy balance model with a 2-box ocean sub-model and IRF tuned to reproduce the response of coupled Earth system models produces a close representation of the globally-averaged temperature response of more complex energy balance models.

1. INTRODUCTION

Worldwide emissions of greenhouse gases (GHGs) and particles from aviation are among the fastest growing sources of human-related forcings on climate (McCarthy, 2010). Aviation contributes to changes in climate forcing directly through emissions of gases like carbon dioxide (CO_2), water vapor, and emissions of particles and particle precursors (e.g., affecting soot and sulfates), indirectly through effects on ozone (O_3) and methane (CH_4) through emissions of nitrogen oxides (NOx), and through increased cloudiness from contrail formation and the particle emissions.

Lee et al. (2009) estimates that aviation contributed approximately 3.5% (range 1.3% to 10%) of the total anthropogenic radiative forcing (RF) on climate for the year 2005 (relative to 1750), excluding the highly uncertain aviation-induced effects on cirrus clouds. CO_2 forcing account for 50% (range 15% to 200%) of this RF and as such, is a major component of aviation forcing. Coupled Earth system models (ESMs) are being used to project the climate effects from natural and human-related emissions including aviation emissions. However, ESMs, while scientifically comprehensive, are computationally expensive, and therefore not ideal for the large number of simulations necessary to address questions of interest to policymakers related to the effects of aviation on climate. As such, development of Simplified Climate Models (SCMs) that can emulate the global averaged results of the more comprehensive climate models on decade to century time scales is important to evaluating policy options and tradeoffs. This would also imply the need for intercomparison studies to assess the behavior of such SCMs and the quality of their projections. Such intercomparisons reported a wide range of model responses to the same emission scenario due to different parameterization of the climate response (e.g., van Vuuren et al. 2009; Warren et al., 2010). In SCMs, the climate response is either parameterized by calibrating a single impulse-response-function (IRF) to the results of more sophisticated parent models, or by calibrating IRFs to dominant physical processes in the system and coupling them to form a non-linear convoluted system model (hereafter called "process specific IRFs"), or by explicitly solving for the dominant processes in the climate system. IRFs are modeled based on linear response theory and are used to reproduce the characteristics of the system response of the sophisticated parent models by assuming a linear response of the system to a perturbation from its equilibrium state. The linear response in this context means, once the IRF's fit coefficients are obtained by calibrating to sophisticated parent models under a specific perturbation, they are fixed regardless of how the background concentration of atmospheric species or other atmospheric states are changing. Previous studies suggest that while IRFs can be used as a surrogate for their parent models within a linear domain, such IRFs degrade in their skill if they are used beyond the linear domain and outside of the original calibration space (Joos et al., 1996 and 2001; Hooss et al., 2001; van Vuuren et al. 2009; Marten, 2011). These studies suggest extending the applicability of these IRFs to the nonlinear domain by explicitly treating the dominant nonlinearities in the climate system. Overall, these studies, as well as other studies such as Thompson and Randerson (1999) and Li et al. (2009), while acknowledging the challenge, suggest the use of such IRFs is justified due to their simplicity. However, they suggest that updating IRFs fit parameters based on more recent generations of ESMs and incorporating dominant nonlinearities in the climate system will improve the skill of such models. Nevertheless, these studies suggest that care must be taken when describing a nonlinear system with a single IRF. Most SCMs that are being used specifically for aviation studies use a single IRF to describe the carbon cycle (for determining changes in atmospheric CO_2 concentration from a given emissions scenario) as they assume CO_2 forcing from aviation is small enough that the system responds linearly. In this paper we discuss the applicability of such assumptions for calculating the change in CO_2 concentration induced by aviation emissions.

The level of parameterization of key interactions is different among different SCMs (e.g., IPCC, 2007). The level of parameterization is a design decision balancing run time, flexibility, and transparency of physical processes versus model complexity and comprehensiveness. In many SCMs, including the ones used in this study, the parameterization methodology is based on using IRFs that have different fit parameters so that the model can represent the range of results from the literature. In light of the importance of SCMs for policy evaluation, the capabilities for representing the carbon cycle and the energy balance model (used to calculate the temperature change resulting from a change in radiative forcing) are intercompared in this study. Six models were selected for this study: the Aviation Environmental Portfolio Management Tool (APMT) model supported by the Federal Aviation Administration (FAA) Partnership for AiR Transportation Noise and Emissions Reduction (PARTNER program (Marais et al., 2008)), two models used at Center for International Climate and Environmental Research-Oslo (CICERO-1 2-box model (Berntsen and Fuglestvedt, 2008) and CICERO-2 upwelling-diffusion energy model (Fuglesvedt and Berntsen, 1999)), the Integrated Science Assessment Model (ISAM) model, the version which has 1-dimension atmosphere, ocean and biosphere (Jain et al., 1994; Jain and Yang, 2005), the simple Linear Climate response (LinClim) model (Lim et al., 2006; Lee et al, 2009), and the Model for the Assessment of Greenhouse-gas Induced Climate Change version 6 (MAGICC6) (Meinshausen et al., 2011). The selected SCMs have different methods for representing the carbon cycle and the Earth's energy balance. The complexity of the representations ranges from relatively simple (APMT, LinClim) to more complex (MAGICC6). Some of these SCMs were specifically designed to evaluate aviation impacts (APMT and LinClim); some were designed for the transportation sectors in general, including aviation (CICERO-1), while others were not and do not directly include aviation (ISAM), or explicitly include aviation (CICERO-2 and MAGICC6). While the distinction of emission location is not important for CO_2 since it is long-lived and well mixed in the atmosphere it is important for other aviation emissions, e.g., NOx, and its effects which are not considered in this work.

A series of three experiments were conducted to compare and evaluate the capabilities of the SCMs' carbon cycle models. The first evaluates the capability of the SCMs to reproduce background CO_2 concentrations by examining the SCM's carbon cycle response to bounding IPCC Fourth Assessment Report (AR4) CO_2 emissions scenarios (IPCC, 2007). The second evaluates the relative importance of different background emission scenarios on the calculation of aviation-induced CO_2 concentrations by examining the SCM's carbon cycle response to a constant year-2000 aviation emission scenario under the different IPCC AR4 background? emission scenarios. The final experiment evaluates the capability of SCMs to project the aviation-induced changes in atmospheric CO_2 by examining the SCM's carbon cycle response to selected background and aviation emission scenarios. A second series of three experiments were conducted to compare and evaluate the capabilities of the SCMs energy balance models. The first examines the energy balance model responses to bounding IPCC AR4 total RF scenarios. The second evaluates the capability of SCMs to project the aviation-induced changes in temperature by examining the SCM's energy balance model response to selected background and aviation RF scenarios. In the following discussion, Section 2 describes the general structure of each SCM and its core components, Section 3 presents the results of the study, and Section 4 summarizes the key conclusions.

2. THE MODELS COMPARED

All of the SCMs included in this study, except MAGICC6 and CICERO-2, calculate global-averaged quantities. MAGICC6 and CICERO-2 both have hemispheric resolution, MAGICC6 calculates the hemispheric land/ocean and globally averaged quantities and CICERO-2 calculates the hemispheric and globally averaged quantities. General descriptions of the carbon cycle and energy models are provided in this section, more detailed descriptions are provided in the supplementary materials.

Carbon cycle models

APMT, CICERO-1 and LinClim calculate the CO_2 concentration resulting from an emission perturbation by using IRFs. However, their IRFs are different as they were calibrated against different parent carbon cycle model and/or under different emission scenarios. ISAM has a complex nonlinear carbon cycle that explicitly treats the CO_2 exchange process within the carbon cycle and CICERO-2 uses interconnected process specific IRFs with explicit treatment of air-sea and air-biosphere exchange of CO_2 (Joos et al., 1996, Alfsen and Berntsen, 1999) that forms a nonlinear carbon cycle. The ocean and biosphere IRFs in CICERO-2 express how the CO_2 impulse decays within each reservoir. The CO_2 partial pressure in each reservoir is calculated as a function of the carbon in that reservoir and the CO_2 partial pressure in each reservoir is related to the CO_2 partial pressure in atmosphere by explicitly solving for the atmosphere-ocean-biosphere CO_2 mass transfer. Therefore, CICERO-2 carbon cycle takes into account the nonlinearity in ocean chemistry and biosphere uptake at high CO_2 partial pressures since it represents the atmospheric change in CO_2 as a function of total background. Similarly, MAGICC6 uses a nonlinear carbon cycle composed of coupled process specific IRFs and is calibrated towards the combined responses of 9 C4MIP carbon cycle models.

Energy balance models

APMT has primarily used the energy balance model developed by Shine et al. (2005) with the purpose of presenting the global temperature potential concept. The Shine et al. (2005) energy balance model assumes that atmosphere exchanges heat only with a slab ocean layer of about 100 m and does not consider the heat transport to the deep ocean. APMT has recently updated its energy balance model based on the results from this study and has now adopted the CICERO-1 energy balance. CICERO-1 uses a 2-box analytical energy balance model composed of an isothermal atmosphere/ocean-mixed-layer box of 70 meters and an isothermal deep ocean box of 3000 meters, and accounts for the heat transfer between the layers (Berntsen and Fuglestvedt, 2008). CICERO2, MAGICC6 and ISAM all have multi-layer ocean sub-models and account for the heat transfer between the layers. CICERO-2 uses the hemispheric energy-balance-climate/upwelling-diffusion-ocean model developed by Schlesinger et al. (1992) to derive hemispheric and globally-averaged temperature changes. It is based on the energy exchange between the atmosphere, ocean mixed-layer, and deep ocean. The mixed-layer thickness is set to 70 meters and the deep ocean is composed of 40 layers with a uniform thickness of 100 meters. MAGICC6 has an upwelling-diffusion energy model for each hemisphere. It has four atmospheric boxes with zero heat capacity, one over land and one over the oceans in each hemisphere. The atmospheric boxes are coupled to the ocean mixed-layer in each hemisphere. The ocean sub-model is composed of a mixed-layer and 39 layers of deep ocean of the same thickness to the total depth of 5000 m. ISAM uses an energy balance model that contains a vertically-integrated atmosphere box, a mixed-layer ocean box, an advective-diffusive deep ocean, and a thin slab representing land thermal inertia. The isothermal mixed-layer depth is 70 meters and is coupled to an advective-diffusive deep ocean composed of 19 layers of varying thickness (Harvey and Schneider, 1985), with higher resolution near the surface due to the larger temperature gradient. The LinClim energy balance model is an IRF based model that has been tuned to reproduce the CMIP3 2xCO2 (equilibrium doubling of CO_2 experiment) behavior of the atmosphere-ocean general circulation model ECHAM5/MPI-OM (Roeckner et al., 2003). More detailed descriptions of SCMs energy balance models are provided in the supplementary materials.

Table 1 lists the main characteristics of each SCM sub-model. All of the SCM simulations in this study were run using a single set of parameters (two sets in the case of APMT). Some of the SCMs used in this study (APMT and MAGICC6) are designed to produce a likely range of climate response. However, the intercomparison presented here is not intended to show an absolute or likely range of climate response, but only how each SCM compares to other SCMs on a similar basis.

3. RESULTS AND DISCUSSION

Intercomparison of carbon cycle models

The carbon cycle is composed of a complex series of processes through which carbon is cycled through different parts of the Earth system. The carbon cycle is a nonlinear system due to nonlinearities in ocean and biosphere uptake of CO_2. At high CO_2 partial pressure (above 50% of preindustrial level (Alfsen and Berntsen, 1999; Joos et al., 1996)) ocean uptake of atmospheric CO_2 decreases due to higher oceanic dissolved CO_2, and less CO_2 is available to be mixed down to the deep ocean by the thermohaline circulation. Biospheric carbon uptake from the increase in net primary production varies proportionally to the logarithm of the atmospheric CO_2 partial pressure and the biosphere release of CO_2 from heterotrophic respiration varies with temperature. Due to the nonlinearities in oceanic and biospheric uptake of CO_2, aviation CO_2 effects over time are determined by calculating the effects of all the human-made sources including aviation (background scenario) and subtracting the effects of all the human-made sources excluding aviation. In this case the calculation of the aviation induced changes in CO_2 concentration is affected by the nonlinearities arising from to the growth of carbon emissions in the background scenario. Therefore, it is important for the carbon cycle models to accurately represent background CO_2 concentrations. Figure 1 shows the carbon cycle response of MAGICC6, CICERO-2, ISAM, and APMT to the IPCC A1FI and B1 SRES bounding CO_2 background emission scenarios relative to the IPCC AR4 mean and the ± 1 standard deviation (SD) range of CO_2 concentration projections taken from IPCC AR4 (IPCC, 2007). The AR4 ± 1 SD range of CO_2 concentration was emulated by calibrating the MAGICC model version 4.2 (Wigley and

Raper, 2001) to a set of carbon cycle models from the "C4MIP" project (hereafter called "± 1 SD range of AR4 CO_2 concentrations") (IPCC, 2007). LinClim and CICERO-1 results are not included in this figure as they do not treat background CO_2 emissions. Their linear IRF carbon cycle models are applied only to aviation CO_2 emissions; background CO_2 emissions are not included in the calculations of the CO_2 concentration. .

The results indicate that all of the SCMs' carbon cycle models except APMT's produce comparable CO_2 concentrations. However, the APMT response to the B1 emission scenario is about 20 ppm higher than the average response from the other models and the mean CO_2 concentration reported in AR4. The APMT response to the A1FI emission scenario is higher than that of the other models and of the mean IPCC up to 2050, and is lower than the other models after 2070, amounting to about 80 ppm lower response at year 2100 compared with the averaged response of the other models. Moreover, results indicate that the projections of all of the models but APMT fall within the ± 1 SD range of AR4 CO_2 concentration projection; however, the APMT results fall outside the AR4 ± 1 SD range for the majority of the simulated time horizon. The reason for such behavior is that APMT uses an IRF for its carbon cycle. The APMT IRF, which is suitable for describing the CO_2 perturbations within the linear region, does not perform as well outside this region (when the increase in atmospheric CO_2 concentration is approximately above 50% of the preindustrial level (e.g., Joos et al., 1996)). The results in Figure 1 indicate that all SCMs that use a nonlinear carbon cycle produce similar CO_2 concentrations. Overall these results are in agreement with those of Warren et al. (2010) who examined the responses of SCM carbon cycle models to SRES emissions scenarios. They found that carbon cycle models with non-linear couplings performed better than those based on a simple IRF formulation.

Figure 2 shows the carbon cycle response of the SCMs to constant annual aviation emissions of 654 Tg CO_2 starting in 2000 (Fuglestvedt et al., 2008) and continuing to 2100, under A1FI, A2, A1B and B1 IPCC background emission scenarios. The results show that both APMT and CICERO-1 produce 4 and 3.8 ppm change in atmospheric CO_2 concentration by 2100, respectively, while LinClim produces about 4.8 ppm change in CO_2 by 2100. This is simply due to the fact that these SCMs have been tuned to different parent models and under different emission scenarios. For all other models the projection of CO_2 concentration at 2100 varies from about 4.3 to about 5.3 ppm. CICERO-2, MAGICC6 and ISAM all produce higher aviation-induced CO_2 concentrations relative to APMT, CICERO-1 and LinClim, and their projections of aviation-induced CO_2 concentration vary in proportion to the growth in the background scenario. The larger the CO_2 emission spread is over time in the background emission scenario, the higher the divergence would be, since due to the nonlinearities in the carbon cycle, higher background carbon emissions would further decrease the ocean and biosphere uptake of additional CO_2 emissions. The increase in spread over time shows the importance of the background scenario on projections of aviation-induced CO_2 concentration. CICERO-1 and LinClim's projection of aviation-induced CO_2 concentration is independent of the background emission scenarios as expected since they do not include the background CO_2 emissions in their calculations. This would be true for any carbon cycle model that uses a simple IRF (i.e. CICERO-1, LinClim, APMT) since they cannot account for non-linear changes in oceanic and biospheric carbon uptake as background carbon changes. Therefore, for carbon cycles that use simple IRFs, the projection of future CO_2 concentration is independent of the CO_2 growth rate in the background emission scenario. Results in Figure 2 indicate that, even though CO_2 emissions from aviation are small compared to overall CO_2 emissions, the simple IRF carbon cycle models are still not appropriate to address the changes in future (~ beyond 50 years in future) CO_2 concentration induced by aviation due to non-linearities in ocean and biosphere uptake of CO_2 which depend on background CO_2 concentrations.

Results in Figure 2 indicate that CICERO-2, MAGICC6 and ISAM produce similar atmospheric CO_2 concentrations, despite the differences in their carbon cycles, as they all account for the nonlinearities in ocean chemistry and biosphere uptake at high CO_2 partial pressure. It is noted that some of the SCMs (i.e. MAGICC6 and ISAM) consider the temperature feedback on carbon cycle (see supplementary materials); but for the time scale and projected temperature change considered in this comparison, the temperature feedback due to incremental changes in aviation CO_2 has a negligible effect on the results presented in this figure (at most 2.5% by 2100).

Figure 3 shows the changes in CO_2 concentration projected by the SCMs relative to IPCC projections obtained from the IPCC Special Report on Aviation and the Global Atmosphere (IPCC, 1999). The comparisons were made for the aviation Edh emission scenario, the high-growth scenario, starting in 1990 and continuing to 2050, with zero emissions afterward, and the

IPCC A1B scenario as the background. The IPCC (1999) analyses of the future change in CO_2 concentration were obtained by calibrating the Wigley (1993) carbon cycle model to the results of ISAM (Jain et al., 1994) and Bern (Siegenthaler and Joos, 1992; Joos et al., 1996) models. The aviation Edh scenario was selected for this comparison since it is the upper bound aviation emission scenario and elucidates the model's responses for the purpose of our comparison. Results show that the projected CO_2 concentrations from APMT and CICERO-1 drop off faster compared to the other models after the emissions stop. LinClim) carbon cycle model produces a higher response compared with APMT and CICERO-1 for the first 80 years and then its projected CO_2 concentrations drop off as fast as APMT and CICERO-1's and falls below MAGICC6, CICERO-2 and ISAM by 2100.

The behavior of these IRFs points to the possibility of finding a particular IRF that provides a close response to a reference case (in this case the IPCC 1999 projections) for emission scenarios inside the original calibration space, but that would not agree as well for a scenario outside the original calibration space (Joos et al., 1996; Meinshausen et al., 2011). The MAGICC6, CICERO-2 and ISAM models produce similar changes in atmospheric CO_2 concentrations as they account for the nonlinearities in ocean chemistry and biosphere uptake. They also produce similar changes in atmospheric CO_2 concentrations compared with IPCC (1999).

Intercomparison of energy balance models

Energy balance models estimate the change in the climate system temperature based on the change in the climate system radiative forcing. In this section the capabilities of the SCMs' energy balance models to calculate the temperature change induced by aviation forcings are compared. For this intercomparision all of the SCMs were run with climate sensitivity of 3 ^{o}C and a mixed-layer depth of 70 meters, which in most models was the default setting, except for APMT which has a default mixed-layer depth of 100 meters, and was run with both a mixed-layer depth of 70 and 100 meters.

Figure 4 presents the temperature response of the SCMs' energy balance models to total radiative forcing from IPCC AR4 A1FI and B1 bounding scenarios obtained from MAGICC model (version 4.2). The temperature responses are compared with the AR4 median and the ± 1 SD range of AR4 temperature projections. The AR4 ± 1 SD range was emulated by calibrating

MAGICC model (version 4.2) to the combined results of C4MIP and the annual average temperature results of 17 coupled atmosphere-ocean general circulation models (AOGCMs) from the "CMIP3" project (hereafter called "± 1 SD range of AR4 temperature") (IPCC, 2007). The AR4 multi-model range for temperature (based on the full temperature range of the 17 AOGCMs that participated in the CMIP3 intercomparison project), is also shown in the grey bars in the right side of Figure 4 for the year 2100.

The APMT, CICERO-1, CICERO-2, LinClim and ISAM energy balance models were forced with RFs from the IPCC AR4 (IPCC, 2007) for total radiative forcing from 1990 to 2100. All of the temperature responses in Figure 4 are relative to year 2000 and the MAGICC6 temperature response is for the respective IPCC AR4 emission scenario, not forced with RFs from the IPCC AR4. However, MAGICC6 calculated RFs for the respective scenarios are within the 2% of the IPCC AR4 RFs. All of the SCMs' temperature responses lie within the AR4 multi-model range for the year 2100 and except for APMT lie within the ± 1 SD range of AR4 temperature projections (Figure 4). APMT produces the largest temperature response for both the A1FI and B1 scenarios among other SCMs. It also produce the highest temperature change compared with the mean and the ± 1 SD range of AR4 temperature projections for both a mixed-layer depth of 70 and 100 meters, and lies at the outer edge or outside of the ± 1 SD range of AR4 temperature projections for most of the simulated time horizon. This is likely due to its use of the single IRF Shine et al. (2005) energy balance model which considers heat transfer to mixed-layer ocean as the sole heat transfer mechanism in the climate system (single timescale). LinClim gives a temperature change consistent with other SCMs that use energy balance models with upwelling-diffusion ocean sub-models even though it uses an IRF energy balance model with multiple timescales.

Figure 5 shows the temperature change derived by the APMT, CICERO-1, CICERO-2, LinClim and ISAM models relative to the temperature change projected by IPCC (1999) by forcing their energy balance model with RFs from the Edh aviation forcing scenario starting at 1990 (IPCC, 1999). The RFs include all aviation forcings. The IPCC (1999) analyses of the future aviation-induced temperature change were obtained by calibrating the upwelling-diffusion, energy balance model of Wigley and Raper (1992) and Raper et al. (1996) to AOGCMs results. MAGICC6 temperature response is to the Edh emission scenario, not forced with RFs from the Edh scenario. The temperature responses in Figure 5 are relative to the year 2000. Forcings before 1990, which were included in the IPCC projection, were not considered in these simulations as there were not reported in IPCC 1999. However, the inclusion of pre-1990 forcings only changes the results slightly (at most 3% if we assume pre-1990 forcings were same as 1990 forcing), and does not affect our conclusions.

All of the SCMs produce a higher temperature change relative to IPCC (1999). However, all of the SCMs but AMPT produce similar aviation-induced temperature change on the time scale of 10-50 years. Results in Figure 5 show that the CICERO-1 energy balance model with a 2-box ocean sub-model and the LinClim temperature IRF that is tuned to ECHAM5 can provide a similar response compared with ISAM and MAGICC6 which utilize upwelling-diffusion ocean sub-models in their energy balance models. APMT produces 33% and 28% higher temperature changes than the other models for mixed-layer depth of 70 and 100 meters, respectively, due to using the Shine et al. (2005) one-box mixed-layer ocean sub-model. The APMT energy balance model with the mixed-layer depth of 70 meters produces about 5% higher temperature change at 2050 than if it were to use a mixed-layer depth of 100 meters.

4. CONCLUSIONS

In this study we compared the capability of six widely used SCMs that were each previously evaluated independently, to project climate effects associated with CO_2 emission from aviation. We have identified several factors that lead to similar performance in some SCMs and that cause some SCMs to be outliers in certain areas. These factors were similar to those previously indicated by other SCMs studies that did not focus on aviation effects (e.g., van Vuuren et al. 2009; Warren et al., 2010). Moreover, our intercomparison resulted in recommendations about how best to represent carbon cycle and energy balance models in SCMs to gauge aviation-induced climate change.

Several factors come into play when choosing a simple climate model to quantify aviation effects on the climate. These factors are the reliability of the representation of the carbon cycle, the energy balance model used to calculate temperature from focing, non-CO_2 emissions effects as well as the capability to project a possible range of future responses and the capability to assess the economic impacts of aviation. While this study focused on the first two of these factors, several of these SCMs (APMT, CICERO-1, CICERO-2, LinClim and MAGICC6), include aviation specific non-CO_2 forcings, e.g., NOx-induced effects and contrails. CICERO-2, MAGICC6, and ISAM have carbon cycle models that include nonlinearities in the ocean and terrestrial biosphere carbon uptake, and therefore are better suited for aviation scenarios outside the linear response regime. The MAGICC6 and CICERO-2 carbon cycle models are simpler than ISAM's; however, since they use IRFs in combination with separate equations describing air-sea and atmosphere-biosphere CO_2 exchange, they extend the use of linear IRFs to the nonlinear domain and give a good approximation (to within 10%) of more complex carbon cycle models.

All of the models used in this study, with the exception of the version of APMT, include either parameterized or explicit calculations of energy exchange with the deep ocean, and hence are expected to perform better for calculations of temperature change, including those from aviation effects. CICERO-1 and LinClim have the simplest energy models that address the heat exchange with the deep ocean. CICERO-1 has a 2 box-ocean sub-model but gives comparable results (to within 10%) to MAGICC6, ISAM, and CICERO-2 that have more complex energy models with upwelling-diffusion ocean sub-models. The LinClim energy balance model is based on an IRF tuned to the ECHAM5 coupled atmosphere ocean general circulation model and can also provide a relatively good (to within 8%) representation of energy balance models with an upwelling-diffusion ocean sub-model.

The ultimate choice of SCM depends on the type of application and the availability of suitable fit parameters for the particular type of application; but it would seem reasonable to include a carbon cycle capable for addressing emission scenarios outside the linear regime and an energy balance model accounting for heat exchange within the deep ocean, as these greatly expand the applicable region in terms of background and future scenarios while adding little computational cost. However, when calculating the impact of all aviation impacts (not just carbon cycle and energy balance models addressed here) it is important that the treatment of those processes is adequately represented. It is noted that depending on the type of application, the ultimate choice of SCM also depends on their capability to provide a possible range of future aviation-induced climate responses, and also, the capability to calculate the economic impacts of aviation. Among the SCMs included in this study, APMT and MAGICC6 are designed to perform Monte Carlo simulations to assess uncertainties of simulated aviation climate impacts, while AMPT is also capable of projecting economic impacts as well as climate impacts.

ACKNOWLEDGMENT

Arezoo Khodayari, Donald J. Wuebbles and Seth Olsen would like to thank the Federal Aviation Administration, Aviation Climate Change Research Initiative (ACCRI) for support under Contract #: 10-C-NE-UI amendment 001 and The Partnership for AiR Transportation Noise and Emissions Reduction (PARTNER). The opinions, findings, and conclusions or recommendations expressed in this material are those of the authors and do not necessarily reflect the views of ACCRI, PARTNER, or the FAA. David S. Lee and Ling L. Lim were partly funded by the UK Department for Transport. Marianne Lund, Jan Fuglestvedt and Terje Berntsen were funded by FAA (ACCRI) and the Norwegian research Council (TEMPO).

REFERENCES

Alfsen, K. H., and T. Berntsen (1999), An efficient and accurate carbon cycle model for use in simple climate models, CICERO, Oslo, Norway.

Berntsen, T., J. S. Fuglestvedt (2008), Global temperature responses to current emissions from the transport sectors, *Proceedings of the National Academy of Sciences*, USA 105, 19154–19159.

Caldeira, K., J. F. Kasting (1993), Insensitivity of Global Warming Potentials to Carbon Dioxide Emission Scenarios, *Nature*, 366: 251-253.

Fuglesvedt, J. S., and T. Berntsen (1999), A simple model for scenario studies of changes in climate, Version 1.0, CICERO, Oslo, Norway, pp. 59.

Fuglestvedt, J. S., T. Berntsen, G. Myhre, K. Rypdal and R. B. Skeie (2008), Climate forcing from the Transport Sectors, *Proceedings of the National Academy of Sciences (PNAS)*, vol 105 (no. 2): pp. 454-458.

Hasselmann, K., R. Sausen, E. Maier-Reimer, R. Voss (1993), On the cold start problem in transient simulations with coupled atmosphere-ocean models, *Climate Dynamics*, Volume 9, Issue 2, 53 – 61.

Hasselmann, K., S. Hasselmann, R. Giering, V. Ocana, H. V. Storch (1997), Sensitivity Study of Optimal CO_2 Emission Paths Using a Simplified Structural Integrated Assessment Model (SIAM), *Climatic Change*, Volume 37, Issue 2, 345 – 386.

Hooss, G., R. Voss, K. Hasselmann, E. Maier-Reimer, F. Joos (2001), A nonlinear impulse response model of the coupled carbon cycle-climate system (NICCS)", *Climate Dynamics*, Volume 18, Issue 3 – 4, 189 – 202.

IPCC (2007), Climate Change 2007: The Physical Science Basis, In: Solomon, S., D. Qin, M. Manning, Z. Chen, M. Marquis, K.B. Averyt, M.Tignor and H.L. Miller (Eds.), Contribution of Working Group I to the Fourth Assessment Report of the IPCC, Cambridge University Press, Cambridge, United Kingdom and New York, NY, USA.

IPCC (1999), Aviation and the global atmosphere, Penner, J. E., D.H. Lister, D.J. Griggs, D.J. Dokken, M. McFarland, (Eds.), Intergovernmental Panel on Climate Change. Cambridge University Press, Cambridge, UK.

IPCC (2012), http://www.ipcc-data.org/ancilliary/tar-bern.txt.

Jain, A. K., and X. Yang (2005), Modeling the effects of two different land cover change data sets on the carbon stocks of plants and soils in concert with CO_2 and climate change. *Global Biogeochemical Cycles*, 19, GB2015, doi:10.1029/2004GB002349.

Jain, A. K., H. S. Kheshgi, and D. J. Wuebbles (1994), Integrated science model for assessment of climate change, UCRL-JC-116526, Lawrence Livermore Nat. Lab., Livermore, Calif.

Jones, C. et al. (2011), The HadGEM2-ES implementation of CMIP5 centennial simulations,

Geoscientific Model Development, 4, 543–570, doi:10.5194/gmd-4-543-2011.

Joos, F., M. Bruno, R. Fink, T. F. Stocker, U. Siegenthaler, C. LeQue´re ´, and J. L. Sarmiento (1996), An efficient and accurate representation of complex oceanic and biospheric models for anthropogenic carbon uptake, *Tellus*, 48B, 397–417.

Joos, F., I. C. Prentice, S. Sitch, R. Meyer, G. Hooss, G. K. Plattner, S. Gerber, K. Hasselmann (2001), Global warming feedbacks on terrestrial carbon uptake under the IPCC emission scenarios, *Global Biogeochemical Cycles*,15, pp. 891–907.

Joos, F., (2002) http://unfccc.int/resource/brazil/carbon.html.

Kheshgi, H. S., A. K. Jain, R. Kotamarthi, D. J. Wuebbles (1999), Future atmospheric methane concentrations in the context of the stabilization of greenhouse gas concentrations, *Journal of Geography Research*, 104, 19,183-19,190.

Kheshgi, H. S., and A. K. Jain (2003), Projecting future climate change: Implications of carbon cycle model intercomparison, *Global Biogeochemical Cycles*, 17(2), 1047, doi: 10.1029/2001GB001842.

Lee, D. S. , D. W. Fahey, P. M. Forster, P. J. Newton, R. C. N. Wit, L. L. Lim, B. Owen, R. Sausen (2009), Aviation and global climate change in the 21st century, *Atmospheric Environment*, doi:10.1016/j.atmosenv.2009.04.024.

Li, S., A. J. Jarvis, D. Leedal (2009), Are response function representations of the global carbon cycle ever interpretable?, *Tellus*, 61B:361–371.

Lim, L., D. S. Lee, R. Sausen, M. Ponater (2007), Quantifying the effects of aviation on radiative forcing and temperature with a climate response model, Proceedings of an International Conference on Transport, Atmosphere and Climate (TAC). Office for Official Publications of the European Communities, Luxembourg, ISBN 92-79-04583-0, pp. 202–207.

Maier-Reimer, E., and K. Hasselmann (1987), Transport & storage of CO_2 in the ocean - an inorganic ocean-circulation carbon cycle model. *Climate Dynamics*, 2, 63 - 90.

McCarthy, J., (2010), Aviation and climate change, in G. Blumenthal (ed.), Aviation and climate change (USA: Nova Science Publishers, Inc.).

Mahashabde, A., et al. (2011), Assessing the environmental impacts of aircraft noise and emissions, *Progress in Aerospace Sciences*, 47, 1, 15-52.

Marais, K., S. P. Lukachko, M. Jun, A. Mahashabde, and I. A. Waitz (2008), Assessing the impact of aviation on climate, *Meteorologische Zeitschrift*, 17(2): 157-172.

Marten, A. L., (2011), Transient Temperature Response Modeling in IAMs: The Effects of Over Simplification on the SCC, *Economics*: The Open-Access, Open-Assessment E-Journal.

Meinshausen, M., S. C. B. Raper and T. M. L. Wigley (2008), Emulating IPCC AR4 atmosphere-ocean and carbon cycle models for projecting global-mean, hemispheric and land/ocean temperatures: MAGICC 6.0, *Atmospheric Chemistry and Physics Discuss*, 8, 6153–6272.

Meinshausen, M., S. C. B. Raper, and T. M. L. Wigley (2011), Emulating coupled atmosphere-ocean and carbon cycle models with a simpler model, MAGICC6 – Part 1: Model description and calibration, *Atmospheric Chemistry and Physics*, 11, 1417–1456, doi:10.5194/acp-11-1417.

Ramaswamy, V., O. Boucher, J. Haigh, D. Hauglustaine, J. Haywood, G. Myhre, T. Nakajima, G. Y. Shi, S. Solomon (2001), Intergovernmental Panel on Climate Change: Chapter 6. Radiative Forcing of Climate Change, In: Climate Change 2001: The Scientific Basis (J. T. Houghton, et al. eds, Cambridge, U.K.: Cambridge University Press).

Raper, S. C. B., T. M. L. Wigley, and R. A. Warrick (1996), Global sea level rise: Past and future. Sea-Level Rise and Coastal Subsidence: Causes, Consequences and Strategies, J. Milliman and B. U. Haq, Eds., *Kluwer Academic*, 11–45.

Roeckner, E, G. Baeuml, L. Bonventura, R. Brokopf, M. Esch, M. Giorgetta, S. Hagemann, I. Kirchner, L. Kornblueh, E. Manzini, A. Rhodin, U. Schlese, U. Schulzweida, and A. Tompkins (2003), The atmospheric general circulation model ECHAM5. PART I: Model description, Report 349, Max Planck Institute for Meteorology, Hamburg, Germany.

Sausen, R., U. Schumann (2000), Estimates of the Climate Response to Aircraft CO_2 and NOx Emissions Scenarios, *Climatic Change*, 44, 1-2, 27-58, DOI 0.1023/A:1005579306109.

Schimel, D., D. Alves, I. Enting, M. Heimann, F. Joos, D. Raynaud and T. Wigley (1996), CO_2 and the carbon cycle, in Climate Change 1995: The Science of Climate Change: Contribution of WGI to the Second Assessment Report of the IPCC, edited by J.T. Houghton et al., pp. 65-86, cambridge University Press, New York.

Sarmiento, J. L., J. C. Orr, and U. Siegenthaler (1992), A perturbation simulation of CO_2 uptake in an ocean general circulation model, *Journal of Geography Research*, 97, 3621–3645, 6163, 6204.

Shine, K. P., J. S. Fuglestvedt, K. Hailemariam, N. Stuber (2005), Alternatives to the global warming potential for comparing climate impacts of emissions of greenhouse gases, *Climatic Change*, Volume 68, Issue 3, Feb, Pages 281 - 302, DOI 10.1007/s10584-005-1146-9.

Siegenthaler, U. and F. Joos (1992), Use of a simple model for studying oceanic tracer distributions and the global carbon cycle, *Tellus*, *44B*, 186-207.

Schlesinger, M. E., X. Jiang, and R. J. Charlson (1992), Implications of anthropogenic atmospheric sulphate for the sensitivity of the climate system, Reprinted form Climate Change and Energy Policy, American Institute of Physics, New York.

Skeie, R. B., J. S. Fuglestvedt, T. Berntsen, M. Lund Tronstad, G. Myhre and K. Rypdal (2009), Global temperature change from the transport sectors: Historical development and future scenarios, *Atmospheric Environment*, 43 (39), pp. 6260-6270.

Thompson, M. V. and J. T. Randerson (1999), Impulse response functions of terrestrial cycle models: method and application, *Global Change Biology*, 5:371–394.

van Vuuren, D. P., J. Lowe, E. Stehfest, L. Gohar, A. F. Hof, C. Hope, R. Warren, M. Meinshausen, G. K. Plattner (2009), How well do integrated assessment models simulate climate change? Climatic Change. doi:10.1007/s10584-009-9764-2.

Warren, R., M. Mastrandrea, C. Hope, and A. Hof (2010), Variation in the climatic response to SRES emissions scenarios in integrated assessment models, *Climatic Change,* 102(3): 671{685. doi:10.1007/s10584-009-9769-x.

Wigley, T. M. L. and S. C. B. Raper (1992), Implications for climate and sea level of revised IPCC emissions scenarios, *Nature*, 357, 293–300.

Wigley, T. M. L. (1993), Balancing the carbon budget: Implications for projections of future carbon dioxide concentration changes, *Tellus*, 45B, 409–425.

Wigley, T. M. L. and S. C. B. Raper (2001), Interpretation of high projections for global-mean warming, *Science*, 293, 451–454.

Harvey, L. D. D., and S. H. Schneider (1985), Transient climate response to External forcing on 100-104 year time scales,1 , Experiment with globally averaged, coupled atmosphere, and ocean energy balance models, *Geophysical Research*, 90, 2191-205.

Lim, L.L., D.S. Lee, R. Sausen, M. Ponater (2006), Quantifying the effects of aviation on radiative forcing and temperature with a climate response model, Proceedings of an International Conference on Transport, Atmosphere and Climate (TAC), Office for Official Publications of the European Communities, Luxembourg, pp. 202–207.

Tabel 1. Characteristic of each SCM sub-models.

Models	**Carbon Cycle Sub-model**	**Energy balance sub-model**	**Feedback between carbon cycle and energy balance sub-models**
APMT	LRF	1-Box	No
CICERO-1	LRF	2-Box	No
CICERO-2	Non-linear Process specific	hemispheric upwelling-diffusion-ocean model	No
ISAM	Non-linear Process specific	upwelling-diffusion-ocean model	Yes
LinClim	LRF	LRF tuned to ECHAM5/MPI-OM $2xCO_2$ experiment	No
MAGICC6	Non-linear Process specific	hemispheric upwelling-diffusion-ocean model	Yes

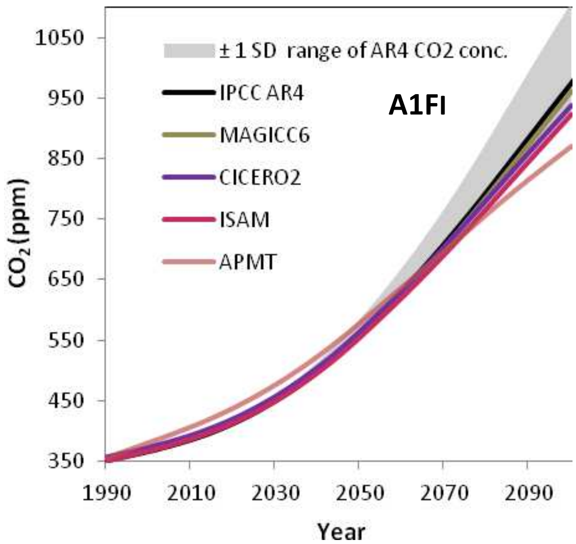

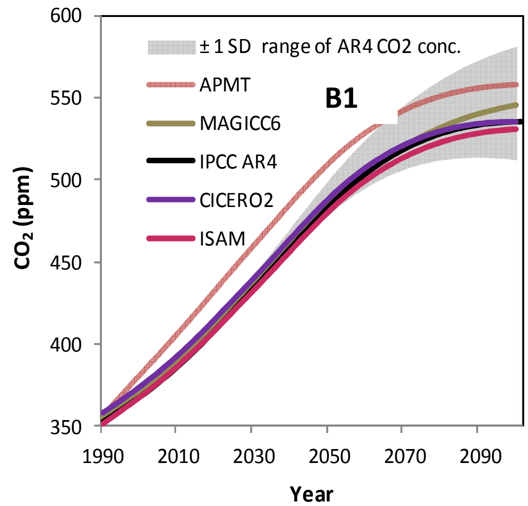

Figure 1. Simple climate model projections of CO_2 concentration for the IPCC SRES A1FI and B1 CO_2 emission scenarios. The mean and ±1 SD of the range of results from the IPCC AR4 projections [IPCC, 2007] are also shown.

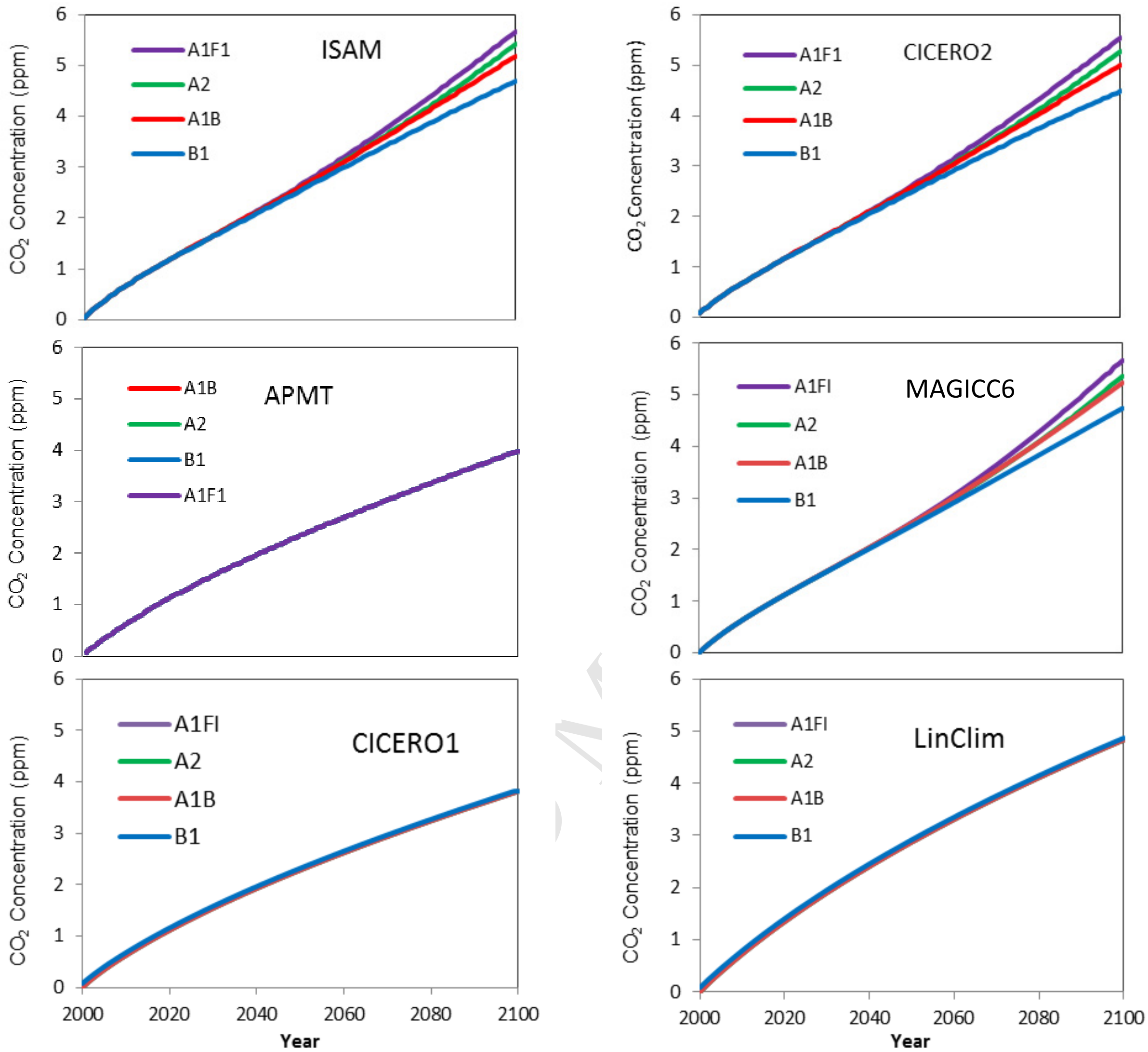

Figure 2. Simple climate model simulated CO_2 concentration for constant CO_2 emissions of 654 Tg/yr (starting in 2000) for different IPCC SRES background CO_2 emissions scenarios.

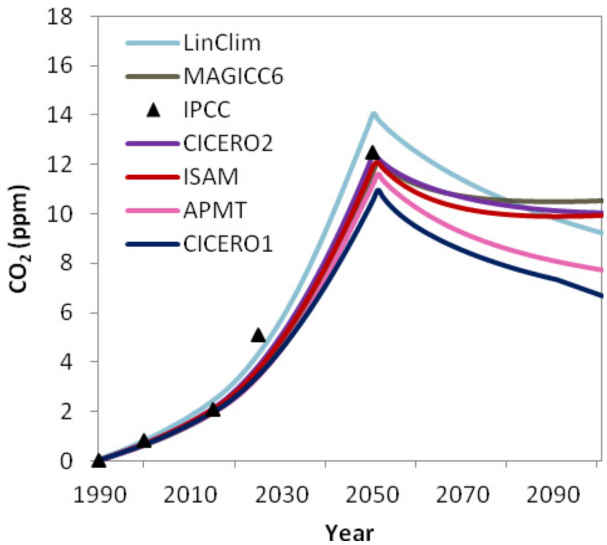

Figure 3. Changes in CO_2 concentrations derived for the APMT, CICERO1, CICERO2, ISAM, LinClim, and MAGICC6 simple models for the CO_2 emissions of Edh aviation scenario up to 2050 and zero emissions afterward and A1B as the background scenario. The IPCC projections [IPCC, 1999] are also shown. The IPCC projection used the IS92a background scenario.

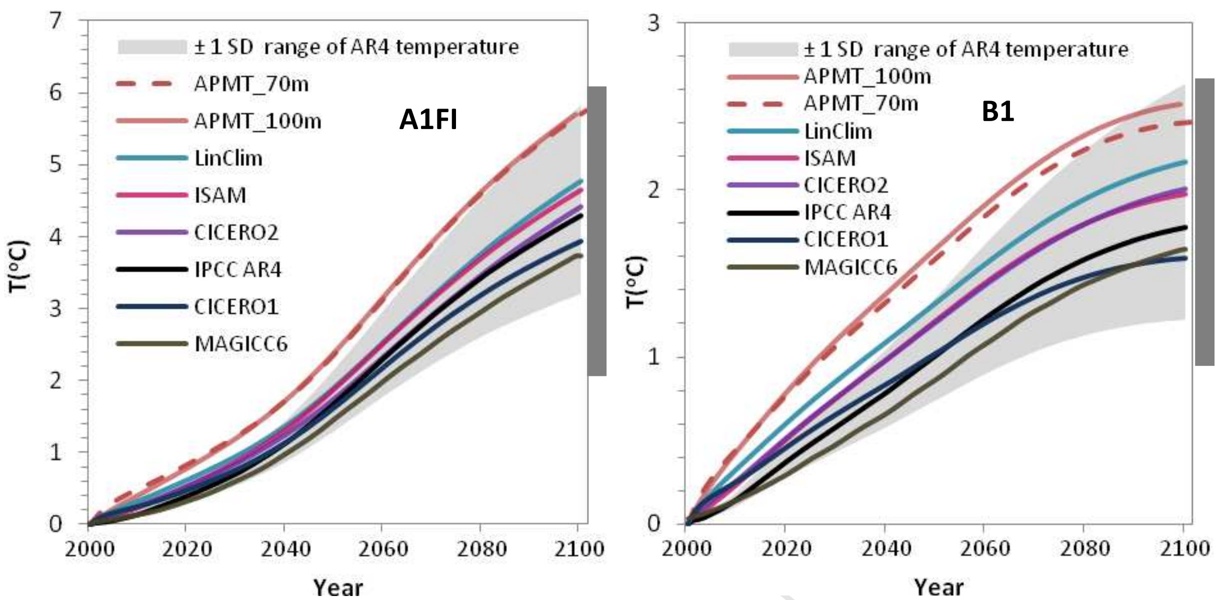

Figure 4. Temperature change (relative to year 2000) projected by APMT, ISAM, CICERO-2, CICERO-1, LinClim, MAGICC6 and IPCC for 2000 to 2100 in response to IPCC AR4 total radiative forcing (Wm^{-2}) (GHG plus direct and indirect aerosol effects) for the A1FI and B1 scenarios. The AR4 multi-model ranges for the year 2100 are shown in the grey bars to the right of the figure.

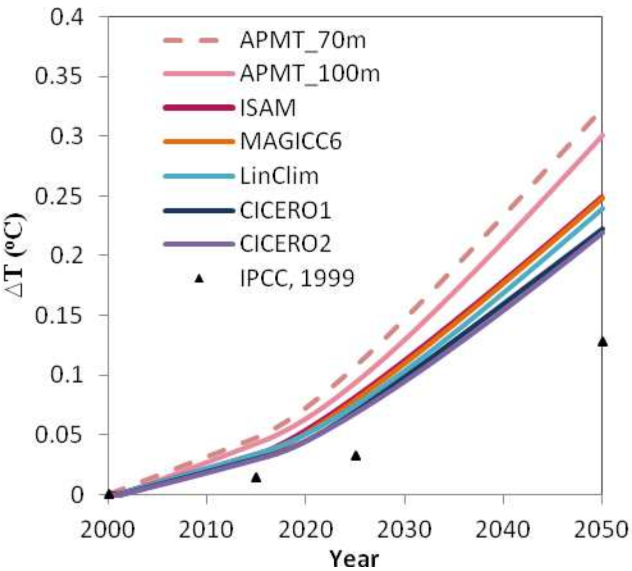

Figure 5. Changes in temperature derived by APMT, CICERO1, CICERO2, ISAM, LinClim and MAGICC simple models relative to IPCC projection [IPCC, 1999]. The SCMs were forced with radiative forcings for Edh aviation scenario from IPCC [1999].

Intercomparision and evaluation of the capabilities of simplified climate models to project the CO_2 effects of aviation on climate

Arezoo Khodayari[a,*], Donald J. Wuebbles[b], Seth Olsen[b], Jan S. Fuglestvedt[c], Terje Berntsen[c], Marianne T. Lund[c], Ian Waitz[d], Philip Wolfe[d], Piers M. Forster[e], Malte Meinshausen[f,g], David S. Lee[h] and Ling L. Lim[h]

[a]Department of Civil and Environmental Engineering, University of Illinois at Urbana-Champaign, Urbana, IL 61801
[b]Department of Atmospheric Sciences, University of Illinois at Urbana-Champaign, Urbana, IL 61801,USA
[c]CICERO, Center for International Climate and Environmental Research, Oslo, P.O. Box 1129, Blindern, 0318 Oslo, Norway
[d]Department of Aeronautics and Astronautics, Massachusetts Institute of Technology, Cambridge, MA 02139, USA
[e]School of Earth and Environment, University of Leeds, LS2 9JT, UK
[f]Earth System Analysis, Potsdam Institute for Climate Impact Research (PIK), Potsdam, Germany
[g] School of Earth Sciences, The University of Melbourne, Victoria 3010, Australia
[h]Dalton Research Institute, Manchester Metropolitan University, UK

* Corresponding author. Tel.: 217-979-3837, E-mail address: akhoday2@illinois.edu

Keywords: climate change, simple climate models, carbon cycle, energy balance model

SUPPLEMENTRY MATERIALS

APMT

APMT was developed to assess both physical climate effects and socio-economic environmental impacts of aviation activity under different aviation scenarios and to capture the uncertainty associated with aviation effects on climate based on a probabilistic approach using Monte-Carlo methods (Mahashabde et al., 2011; Marais et al., 2008). Typically, APMT runs probabilistically for a policy scenario paired with a baseline scenario. This approach can be used to more accurately represent the uncertainties in outputs by formally accounting for the reduced influence of modeling uncertainties that are common to both the policy and baseline scenarios. In this study, deterministic analyses were used for evaluation of APMT compared with other SCMs as the purpose is to evaluate the underlying physical structure and capabilities of the models.

Therefore, while this analysis provides a good indication of the uncertainties and biases in the underlying sub-models, it does not provide an indication of the uncertainties or biases in the overall APMT-Impacts climate model when it is run probabilistically to represent a range of results from the literature (the task for which it was designed).

APMT calculates the CO_2 concentration resulting from an emission perturbation by using a linear-response-function (LRF) (Marais et al., 2008). LRF is "defined as the CO_2 signal observed in the atmosphere for a δ-function atmospheric input at time t=0 (or equivalently a unit step-function change in the initial atmospheric CO_2 concentration)" (Maier-Reimer and Hasselmann, 1987). LRF is derived from an exponential curve fit to the change in atmospheric CO_2 concentration as a function of time for a certain CO_2 emission pulse. The CO_2 concentrations used for this fit result from simulations with a three-dimensional coupled model of the Earth's system. By default, APMT uses the Bern atmospheric LRF (Joos et al., 1996) that was derived by calibration against the Bern carbon cycle model under a baseline scenario that is an instantaneous release of 1 ppm CO_2 into the background atmosphere with 378 ppm CO_2 (IPCC, 2007). APMT also has the option of using other atmospheric LRFs, including Hasselmann et al. (1993), Hasselmann et al. (1997) and Hooss et al. (2001). These atmospheric LRFs have a same form as the default Bern LRF with different coefficients. These carbon cycle models are not utilized in APMT during a typical policy analysis as they are older LRFs that are not representative of current scientific understanding, but they are included in the model to provide flexibility to directly compare APMT to other SCMs.

The radiative forcing on climate derived for aviation-emitted CO_2 in APMT as well as all other SCMs except CICERO-1, is calculated explicitly based on the following simplified function as described by IPCC Third Assessment Report (Ramaswamy et al., 2001).

$$RF_{CO_2} = \alpha_{CO_2} \ln\left(C / C_0 \right) \tag{1}$$

Where RF_{CO_2} is the adjusted radiative forcing from CO_2 (Wm^{-2}) for a CO_2 concentration C (ppm) above the preindustrial concentration C_0 (278 ppm). The scaling parameter α_{CO_2} has the value of 5.35 Wm^{-2} (=$\frac{3.71}{\ln(2)}$ Wm^{-2}).

To calculate the temperature change for a given change in radiative forcing, APMT has primarily used the energy balance model developed by Shine et al. (2005) with the purpose of presenting the global temperature potential concept. The Shine et al. energy balance model assumes the heat capacity of the earth resides in a 100 m deep ocean mixed-layer with a heat capacity of 4.2×10^{8} $JK^{-1}m^{-2}$ with no deeper ocean layers. APMT has recently updated its energy balance model based on the results from this study and has now adopted the CICERO-1 energy balance model that will be explained in detail in the CICERO-1 section.

CICERO-1

CICERO-1 was developed to compare the relative physical climate effect of different transportation sectors (road, ship, air, and rail) over the next century (Berntsen and Fuglestvedt, 2008).

Like APMT, CICERO-1 employs the Joos et al. (1996) LRF to describe the relation between CO_2 emissions and atmospheric concentrations adopted from IPCC third assessment report (TAR). The coefficients are derived by calibration against the Bern carbon cycle model, but under a different baseline scenario than the LRFs used by APMT; namely, it is based on an instantaneous release of 40 GTC input into the preindustrial atmosphere (Joos, 2002). CICERO-1 uses a constant specific radiative forcing for CO_2 over time of 1.8×10^{-15} $W/m^2/Kg\ CO_2$ (Caldeira and Kasting, 1993).

CICERO-1 uses a 2-box analytical energy balance model composed of an isothermal atmosphere/ocean-mixed-layer box of 70 meters and an isothermal deep ocean box 3000 meters (Berntsen and Fuglestvedt, 2008). Heat transfer between the two layers is represented by a constant advective water mass flux of 1.23×10^{-4} $kgm^{-2}s^{-1}$ from the mixed-layer to the deep ocean, and a turbulent diffusive heat transfer between layers with a diffusion coefficient of 4.4×10^{-5} m^2s^{-1}. The heat capacities for the ocean mixed-layer and deep ocean are $2.94\times10^{8}Jk^{-1}m^{-2}$ and 1.26×10^{10} $JK^{-1}m^{-2}$, respectively (Berntsen and Fuglestvedt, 2008). It is noted that the constant parameters used in CICERO-1 energy balance model were obtained by tuning to an ESM.

CICER0-2

CICERO-2 was implemented to estimate the climate effect of anthropogenic emissions, including the aviation sector, under different emission scenarios (Fuglesvedt and Berntsen, 1999; Skeie et al. 2009). The CICERO-2 carbon cycle is based on the approach by Joos et al. (1996) which simulates the dynamics of a three-box atmosphere-ocean-biosphere system. It uses process specific LRFs for each reservoir (ocean and biosphere) to express the decay of CO_2 impulse in each reservoir, and then calculates the CO_2 partial pressure at each reservoir as a function of total background carbon in each reservoir (Alfsen and Berntsen, 1999), and finally interconnects the CO_2 partial pressure in ocean and biosphere to the CO_2 partial pressure in atmosphere by explicit treatment of atmosphere-ocean-biosphere mass transfer of CO_2 to account for the nonlinearities in the system. Therefore, its carbon cycle takes into account the nonlinearities in the system as it represents the change in atmospheric CO_2 as a function of total background carbon. The ocean LRF, which represents the mixed-layer carbon content, is calibrated against the HILDA model (Joos et al., 1996). The correlation between mixed-layer background inorganic carbon content and mixed-layer CO_2 partial pressure was calibrated against the three-dimensional Bern carbon cycle (Joos et al., 2001). CICERO-2 accounts for the biosphere response by considering the CO_2 uptake and release of terrestrial vegetation as a function of the CO_2 fertilization effect. The increase in the rate of photosynthesis, relative to preindustrial times, is considered to be proportional to the logarithm of the relative increase in atmospheric CO_2 concentration from its pre-industrial value of 278 ppm. The proportionality constant, known as the CO_2 fertilization factor, is 0.287. CICERO-2 accounts for the feedback of carbon on the carbon cycle through changes in biosphere fertilization and through changes in ocean chemistry.

CICERO-2 uses the hemispheric energy-balance-climate/upwelling-diffusion-ocean model developed by Schlesinger et al. (1992) to derive hemispheric and globally-averaged temperature changes. It is based on the energy exchange between the atmosphere, ocean mixed-layer, and deep ocean. The atmosphere is divided into two boxes in each hemisphere, one over land and one over ocean. The mixed-layer thickness is set to 70 meters and the deep ocean is composed of 40 layers with a uniform thickness of 100 meters. The ocean is subdivided horizontally into the polar region, where bottom water is formed and is recirculated to complete the thermohaline circulation, and the nonpolar region, where there is upwelling. In the nonpolar region, heat is transported upward by upwelling and downward by physical processes the effects of which are considered as an equivalent diffusion. Moreover, heat is also moved from the mixed-layer in the nonpolar region to the polar region, and from there it is transported to the bottom by downwelling. This heat is ultimately transported upward from the ocean floor in the nonpolar region. Vertical upwelling and thermal diffusion happen over the deep ocean with uniform upwelling velocity of $4 myr^{-1}$ and uniform vertical thermal diffusivity of $0.227\ m^2yr^{-1}$. CICERO-2 calculates the global mean temperature change and the individual change in temperature over sea and land in each hemisphere (Andronova and Schlesinger, 2001).

ISAM

ISAM was originally developed to estimate the past carbon budget given past CO_2 concentration, fossil carbon emission, and temperature records, and also to estimate the climate effect of anthropogenic emissions under different emission scenarios (Kheshgi and Jain, 2003). Different versions of ISAM were used to study the effect of CO_2 and climate change on ocean acidification and carbon sequestration in agricultural soils, and also to study the biophysical effect of bioenergy production. ISAM was used for future climate projections from emission scenarios in both the IPCC second assessment report (SAR) (Schimel et al., 1996) and third assessment report (TAR) (Ramaswamy et al., 2001).

The ISAM carbon cycle consists of a simplified one box atmosphere which is coupled to a six-box globally aggregated terrestrial biosphere sub-model that represents ground vegetation, non-woody tree parts, woody tree parts, detritus, mobile soil (turn-over time 75 years), resistant soil (turnover time 500 years); an ocean mixed-layer and a vertically resolved advective-diffusion deep ocean. Air-sea exchange is modeled by an air-sea exchange coefficient in combination with the buffer factor that summarizes the chemical re-equilibration of sea water with respect to CO_2 variations (Jain et al., 1995), and as such accounts for the nonlinearity in ocean chemistry at high CO_2 partial pressures. ISAM has a one-dimensional column ocean that is treated as a mixed-layer with a depth of 70 m, and a deep ocean with a depth of 4000 m that is composed of 40 layers. The transport in the ocean takes place through the thermohaline circulation and depends on upwelling velocity of 3.5 m/yr and eddy diffusivity of 4700 m^2/yr resulting from calibration to the estimated global-mean pre-anthropogenic depth-profile of ocean ^{14}C concentration (Jain et al., 1995). The increase in the rate of photosynthesis, relative to preindustrial times, is modeled to be proportional to the logarithm of the relative increase in atmospheric CO_2 concentration from its pre-industrial value of 278 ppm. The proportionality constant, known as the CO_2 fertilization factor, is 0.45. (Kheshgi and Jain, 2003).

ISAM uses an energy balance model that contains a vertically-integrated atmosphere box, a mixed-layer ocean box, an advective-diffusive deep ocean, and a thin slab representing land thermal inertia. The isothermal mixed-layer depth is 70 meters and is coupled to an advective-diffusive deep ocean composed of 19 layers of varying thickness (Harvey and Schneider, 1985), with higher resolution near the surface due to the larger temperature gradient. Thermohaline circulation is represented by an advective heat transport between the layers. There is also a diffusive heat transfer term that accounts for small-scale vertical mixing. Thermal diffusivity and upwelling velocity are 0.216 m^2yr^{-1} and 4 myr^{-1}, respectively, and are constant with respect to ocean depth.

There is a coupling between the carbon cycle and the energy balance model in ISAM that accounts for the feedback of climate change on the carbon cycle. ISAM also accounts for carbon feedback on the carbon cycle through the changes in biosphere fertilization and oceanic CO_2 uptake.

LinClim

LinClim (Lim et al., 2007; Lee et al., 2009) is a simplified climate response model, which has expanded the approach presented in Sausen and Schumann (2000), to include the full suite of aviation-specific effects identified by IPCC (1999).

LinClim first derives aviation CO_2 emissions from fuel data. It then calculates CO_2 concentrations resulting from the aviation emissions by using the Hasselmann et al. (1997) LRF. The current version of LinClim uses fit parameters which approximates the results of the Maier-Reimer and Hasselmann (1987) carbon-cycle model.

The simplified expression published in IPCC (2007) is used to calculate CO_2 RF. However, in order to calculate the contribution of aviation CO_2 to RF, LinClim also requires background CO_2 concentration. Historical background CO_2 concentrations are obtained from IPCC observed concentrations, while future concentrations are obtained from other carbon-cycle models or published data. The aviation CO_2 RF is then assumed to be the difference between background RF and RF due to the difference between background and aviation concentrations. In this study, the background concentrations were obtained from the IPCC BERN data (IPCC, 2012).

The temperature response in LinClim is defined by a LRF derived by Hasselmann et al., (1993). The formulation has since been expanded to include the perturbation's efficacy (Lim et al., 2007). This LRF can be tuned to climate models running different types of experiments. There is no constraint on the number of degrees of freedom. Therefore, when tuned, the temperature response is able to approximate the full results of the parent climate model and type of experiment, fully capturing the simulations. At present, LinClim has been tuned to numerous climate models (ECHAM4, CNRM, UM, CMIP3 (phase 3 of the Coupled Model Intercomparison Project, IPCC, 2007) models), running different types of experiments (pulse, transient, $2xCO_2$ and $4xCO_2$). In this study, the temperature LRF has been tuned to reproduce the CMIP3 2xCO2 (equilibrium doubling of CO_2 experiment) behavior of the atmosphere-ocean general circulation model ECHAM5/MPI-OM (Roeckner et al., 2003).

MAGICC6

MAGICC was developed to emulate the results of ESMs and it was used in previous IPCC reports for various scenario analyses (Meinshausen et al., 2008). It combines the carbon cycle response calibration to 9 C4MIP (Coupled Carbon Cycle Climate Model Intercomparison Project) models and climate response calibration to 19 AOGCMs (Atmosphere/Ocean General Circulation Models) that were included in CMIP3.

The MAGICC6 carbon cycle consists of a homogenous atmosphere coupled to a three-box globally aggregated terrestrial biosphere sub-model that represents a living plant box and two dead biomass boxes of detritus and organic matter in soils; and an ocean sub-model. The detail of this carbon cycle is described in (Meinshausen et al., 2011), and same as CICERO-2 carbon cycle, it uses process specific LRFs that are interconnected in order to form a nonlinear carbon cycle model. The ocean sub-model in the MAGICC6 carbon cycle has the same applied analytical representation of LRF as used in CICERO-2 (Joos et al., 2001). However, the difference is that the mixed-layer LRF in MAGICC6 is calibrated against the 3-D-GFDL model (Sarmiento et al., 1992).

MAGICC6 accounts for the atmospheric CO_2 fertilization effect on net primary production. The increase in net photosynthesis due to the CO_2 fertilization effect is modeled as a linear combination of both a logarithmic form and a rectangular hyperbolic form. This is more realistic than the logarithmic form of the relative increase in atmospheric CO_2 concentration used in CICERO-2 and ISAM for both high and low CO_2 concentration as the net primary production does not rise without limit as CO_2 concentrations increase (Meinshausen et al., 2011).

MAGICC6 has an upwelling-diffusion energy model for each hemisphere. It has four boxes with zero heat capacity, one over land and one over the oceans in each hemisphere. The atmospheric boxes are coupled to the ocean mixed-layer in each hemisphere. The ocean sub-model is composed of a mixed-layer and 39 layers of deep ocean of the same thickness to the total depth of 5000 m. Ocean area, upwelling and diffusion throughout the oceans are temperature and depth dependent (Meinshausen et al., 2011). The assumption of constant upwelling and diffusion in the ocean sub-model can lead to an overestimate of the ocean heat uptake for higher warming scenarios if parameter values are based on calibration to lower warming scenarios. However, the temperature-dependent representation of upwelling and diffusion decreases the heat uptake due to thermal stratification and reduced vertical mixing in the higher warming scenarios. The MAGGIC6 energy model has time-varying effective climate sensitivities that are a function of climate state. The change in effective climate sensitivity over time results from the modification of land-ocean heat exchange. MAGICC6 accounts for the feedbacks of both carbon and climate on carbon cycle.